

Article

Techno-Economic Feasibility of Hybrid Solar Photovoltaic and Battery Energy Storage Power System for a Soshanguve Mobile Cellular Base Station in South Africa

Banjo A. Aderemi¹, SP Daniel Chowdhury², Thomas O. Olwal³, Adnan M. Abu-Mahfouz⁴

¹⁻⁴ Department of Electrical Engineering, Tshwane University of Technology Pretoria, South Africa.

⁴ CSIR Meraka Institute Pretoria, South Africa.

[1ayoadebanjo93@hotmail.com](mailto:ayoadebanjo93@hotmail.com), [2spchowdhury2010@gmail.com](mailto:spchowdhury2010@gmail.com), [3olwalto@tut.ac.za](mailto:olwalto@tut.ac.za), [4a.abumahfouz@ieee.org](mailto:a.abumahfouz@ieee.org)

Abstract: Over the years, sustainability, impact on the environment, as well as the operation expenditure have been a major concern to the deployment of mobile cellular base stations worldwide. This is because the mobile cellular base stations are known to consume a high percentage of power within the mobile cellular network. Such energy consumption contributes to the emission of Greenhouse Gases (GHG) through the use of conventional diesel generating a set. As a result, the mobile cellular operators are faced with the dilemma of minimising the power consumption, GHG emission, and the operation cost, while improving the Quality of Service of the networks. In attempting to find a solution, this study presents the feasibility and simulation of a solar photovoltaic (PV) with battery hybrid power system (HPS) as a predominant source of power for a specific mobile cellular base station site situated in Soshanguve area of the city of Pretoria, South Africa. It also presents the technical development, showed the environmental advantage and cost benefits of using a solar PV-battery HPS to power a base station site of a 24 hrs daily load of 241.10 kWh/d and the peak load of 20.31 kW as compared to using the HPS of solar PV-diesel generating set-battery. The solar resource pattern for the city of Pretoria was collected from The National Aeronautics and Space Administration and modelled statistically. Thus, the statistical modelling done using solar radiation resource exposure characteristic patterns of Pretoria, South Africa, revealed an average annual daily solar radiation of 5.4645 Wh/m²/d and 0.605 clearness index. The simulation and the design were done using the Hybrid Optimization Model for Electric Renewables and Matlab/Simulink software. The simulation finding shows that the HPS of solar PV-battery combination has about 59.62 % saving on Net Present Cost, Levelized Cost of Energy, and 80.87% saving on Operating cost as against conventional BS powered with Gen Set-Battery.

Keywords: Solar PV, Green Energy, Hybrid Power Source, Mobile Cellular Base Station, OPEX, Solar Irradiance

1. Introduction

Growth in the use of mobile cellular communication worldwide has led to an increase in the electrical consumption in the mobile telecommunication industries to about 10% between the year 2013 and 2018 [1], [2], [3], [4], and [5]. According to [6], mobile cellular base stations (BSs), primarily contribute about 60% of the total electrical power consumption within the mobile cellular networks. Consequently, given the rise in the number of BSs daily, there is a corresponding rise in the Operational Expenditure (OPEX), to an estimation of multiple of ten times [7]. Parallel to this increase in cost, the level of Greenhouse Gases (GHGs) emission will also experience a direct increase of about three factors between the year 2007 to 2020 [8]. Often cited to support the increase in GHG emission is a report of GHG emissions by Standards, Monitoring, Accounting, Rethink, Transform (SMART), 2020 [9].

Apart from the high rate of mobile service subscribers in an urban area, rural areas are now experiencing a significant increase in the number of subscribers to mobile cellular services. Globally, there

was the addition of about 1 billion new subscribers to the mobile cellular service from the rural areas between the year 1997 and 2012 [3]. Therefore, to increase their rural capacity, coverage, and profit, mobile cellular service providers are augmenting their services through installation of new mobile cellular BSs to join the existing ones [10]. It is estimated that there are over 4 million deployed mobile cellular BSs across the globe, however, most of them are powered using diesel generating set as standalone in rural areas due to lack of dependable grid system, thus, leading to increases in GHG emission, and higher cost of OPEX [11, 12]. This is because irregular power and lack of dependable functioning grid system affect the supply of electrical energy to these BSs in most part of developing countries. Hence, lack of regular uninterrupted power supply could limit the BSs from been able to discharge its minimum required Quality of Service (QoS) to the satisfaction of the subscribers [6]. In addition to this, reduction in the BSs' QoS is caused as a result of overloading and high power consumption [13, 14]. To solve these challenges mentioned especially in the rural area, there is a need for uninterrupted, reliable, efficient, cost-effective, and environmentally friendly power supply.

Among various attempts to solve the aforementioned problem, is the global deployment of diesel generating set at rural BSs. Because of global warming, air pollution, lack of reliability, high operational and maintenance costs (O&M), low efficiency, high total cost of ownership (TCO), and unavailability, the attempt to use diesel generating set as the main power source have become unattractive [15-17]. The use of the renewable hybrid power source method is now becoming attractive because of prominent features such as sustainability, reliability; cost-efficiency, environmental benefits, and guarantee the return on investment. Through the utilization of advanced solar technology, these important key features can be met. Solar energy is clean, available in abundance, free in nature, and accessible through the season, hence, why this study explores it. Another factor considered is the solar exposure patterns such as radiation, temperature, and intensity of the location.

This study aims to investigate the techno-economic feasibility of adopting an HPS of solar-PV-battery arrangement for a mobile cellular base station (BS), a site located in Soshanguve rural area. The statistical modelling and simulation were based on the average daily South Africa solar radiation exposure pattern. Using the Hybrid Optimization Model for Electric Renewables (HOMER) simulation software, this article presents both the economic and environmental impacts of using the HPS model in this area. However, the main contributions of this study are:

- The feasibility study of solar PV power system under different average daily solar exposure pattern of this location to generate sufficient power to feed the mobile cellular BS;
- Using HOMER software, both the technical and economic feasibilities of using this proposed hybrid power system were determined;
- Environmental and economic comparison of this proposed hybrid power system against the conventional use of a diesel generating set.

The arrangement of this paper is as follows; section 2 discusses the overview of the system components and system modelling. The methodology used is stated in section 3, section 4 discusses the result, while Section 5 contains the conclusion.

2. Overview and System Modelling

The aim of this section is to provide the architecture and design of the major components of the solar PV powered BS and their mathematical models.

2.1. Solar PV Powered System Architecture

Consider the Figure 1 which stands for a block diagram of a typical BS powered by the hybrid power system. It is made up of two systems namely; hybrid energy sources and the mobile cellular BS. In this system, the HSP supplies the power needed to the BS based on the available energy resource from the solar PV, the battery or the diesel generating set controls by the flowchart in Figure 2. The mobile cellular BS system, as illustrated in Figure 1 is a direct current (DC), the load which is fed directly by solar PV modules. The excess electrical energy is stored in the array of the battery bank. Both the battery bank and diesel genset/grid system compensates for any discrepancy in energy level from the solar PV system. Figure 2 describes the power management operation of this hybrid system. It also gives the power source control management algorithm flow chat module. The purpose of this algorithm is to orchestrate constant supply of power to the mobile cellular BS without any downtime in the operation of BS from the HPS. It also manages the proper use of energy harvested by the solar PV panels. The solar power is seen as the most appropriate energy harvesting technology because of its global availability, and good quality performance of the photovoltaic (PV) panels. Although the use of solar PV to power mobile cellular BS started with second generation (2G) technology, its utilization is mostly in the rural area where there is no access to grid system [18]. Nonetheless, the solar PV powered BS is becoming widely accepted in the urban area thanks to a reduction in OPEX, advancement in renewable energy research, and viability of new BSs with low power consumption and less space[19, 20].

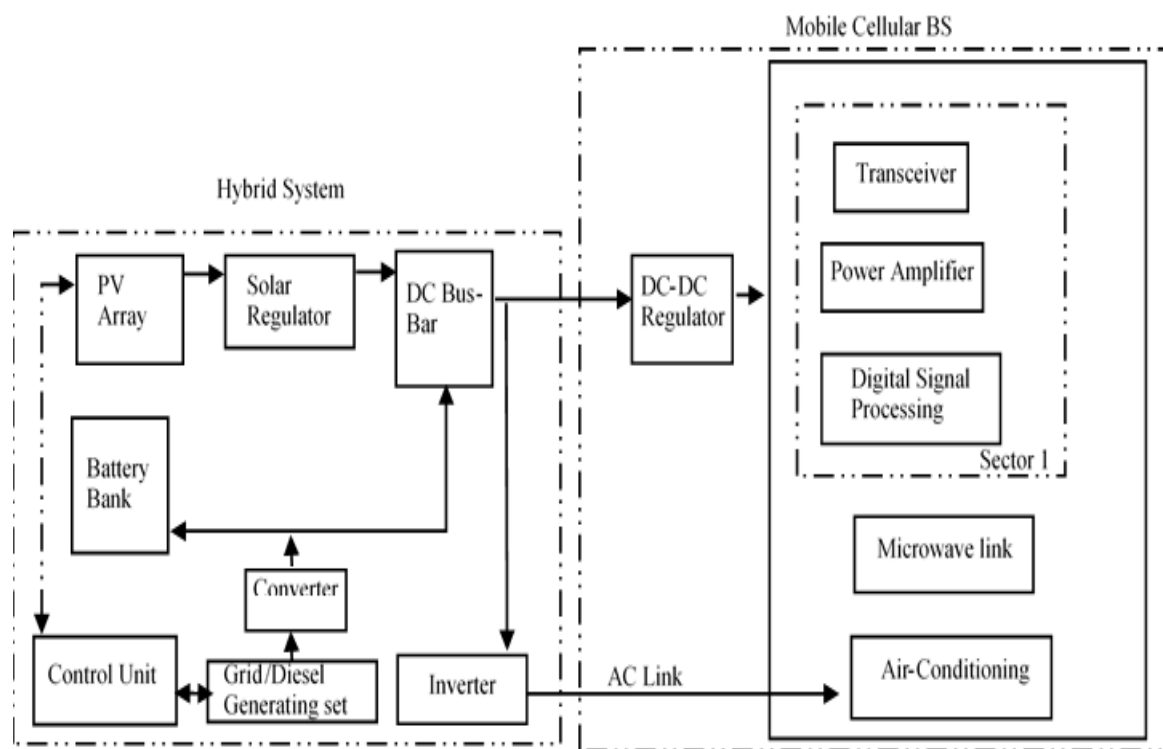


Figure 1. Hybrid Power System Powered Mobile Cellular Base Station [21].

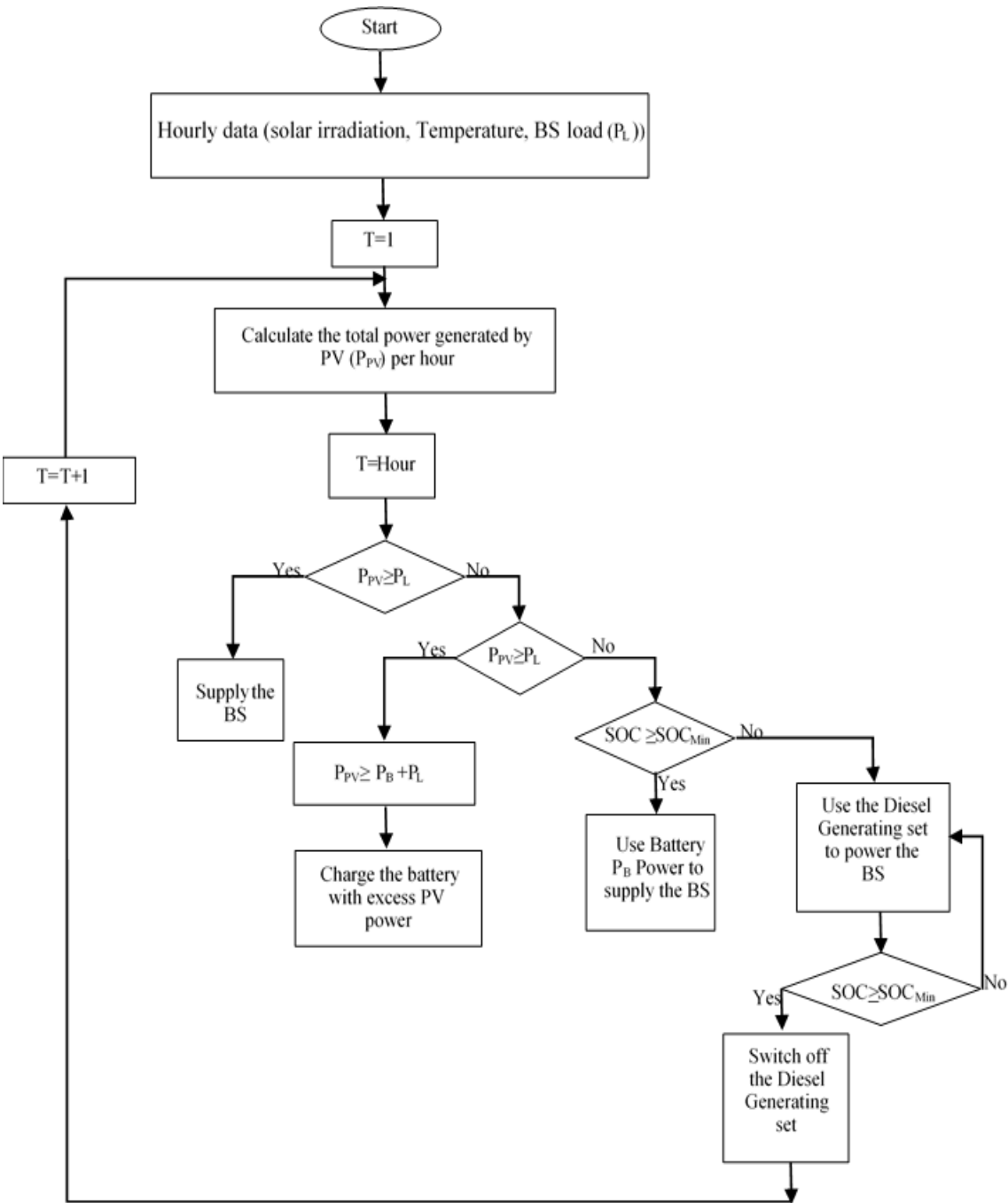


Figure 2. Hybrid Power System Management Algorithm flow chat.

2.2. Mathematical Models for Hybrid Power System

The goal of this section is to provide insight into the mathematically formulated models used in determining the relationship between all the components such as the BS, the HPS, and the costs in this hybrid power system. While the cost mathematical models assist to estimates the life-cycle cost of the system and its advantages, the other system element models ensure energy management balance between the energy delivered by the HPS and the energy required by the mobile cellular BS.

2.2.1. Mobile Cellular BS Modelling

According to [16, 22, 23], BS can be described as a link which provides a direct path from the mobile core network to the mobile stations covering various cells. The solar PV panel can power the BS directly because the BS is primarily a DC load which comprises mainly power amplifiers (PA), transceiver (RF), the baseband unit (BB), microwave backhaul, and auxiliary equipment such as lighting, air conditioning [23], as shown in Figure 1. Figure 3 shows the percentage of power consumption in each unit of mobile cellular BS shown in Figure 1. There are several types of mobile cellular BS such as Macro BS, Micro BS, Femto BS, and Pico BS. These BSs are categorized based on their size and power consumption. Of all these BSs mentioned, Macro BS is the most commonly used BS [6]. The total power requirement of the site was calculated using [24].

$$P = \sum_{n=1}^N P_n \times \frac{T_n}{24} \quad (1)$$

Where P is the total capacity of the BS DC load power, P_n is the energy consumption of all the equipment on site, and T_n represent the corresponding run time of the equipment energy.

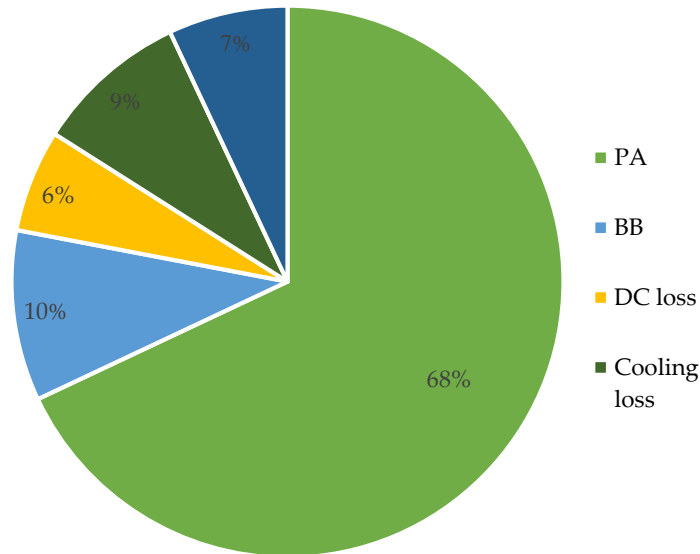


Figure 3. Percentage of power consumption in a Macro BS [22].

As given in [22, 23, 25, 26], macro BS models power consumption by (2);

$$P_{BS} = N_{TRX}(P_o + \Delta_p P_{max} K), 0 \leq K \leq 1 \quad (2)$$

In (2), N_{TRX} is the total number of transceivers, at zero traffic or no load, P_o is the power consumed ranges from 118.7 W and above, the BS manufacturer represents BS constant by Δ_p , its value ranges from 2.66. The power amplifier at maximum load or traffic is given by P_{max} , its value also ranges from 40 W and above for a macro mobile cellular BS. While the normalized traffic at a given time is represented by K . From (1), the power consumes by a BS depends on the traffic load depending on the time of the day. Thus, the normalized traffic load for a BS at any given time is modelled by [27] as

$$K(t) = N_t / N_{max} \quad (3)$$

In (3), at any time, the number of active traffic load is N_t , while at any spectrum distributed to the BS, the most number of users allowed by the BS at any given normalized time is N_{max} .

2.2.2. Hybrid System Modelling

Hybrid power system consists solar PV panels, the batteries, converter, and power back such as grid or diesel generating set as seen in Figure 1. The mathematical models for each one of them are based on HOMER models as given by [28] which are used to calculate the simulation parameters used in this study.

2.2.3. Solar PV Arrays Model

Solar PV array is a combination of many interconnecting different solar modules formed through the fusion of many solar cells. The PV panels are rated in direct current (DC), based on the power it can generate when the solar power available on it power is 1 kW/m². Presently, commonly used PV cells with an efficiency of about 15-19 percent are mono and polycrystalline silicon, in large-scale applications [6, 29]. According to [12, 30], the output power of the PV modules is determined by the PV cell material, the cell temperature, the solar radiation incident on the PV modules, the DC-AC loss factor, the tilt of the PV panel as well as the geographical location of the site. [31-33] explained that these solar cells act as a membrane which attracts and convert short irradiance wave to a DC electricity. Mathematically, HOMER proved the yearly total energy produced by solar PV array using (4), based on equations by [21].

$$E_{PV} = Y_{PV} \times PSH \times f_{PV} \times 365 \text{ day/year} \quad (4)$$

From (4), the peak capacity of the PV array measured in kW is represented by Y_{PV} . The average daily solar radiation is the Peak Solar Hour (PSH), measured per hour. Other factors such as dust, temperature, wire losses that can affect the wattage output of the solar PV is expressed as the PV derating factor f_{PV} . The overall efficiency of the solar PV modules is called the derating factor. These PV arrays are interconnected in parallel-series configuration and grouped together in a unit to form what is referred to as solar PV module. Therefore, through the use of KVL in (5), the output current I can be estimated in Matlab/Simulink.

$$I = I_L - I_d - \frac{V_o}{R_{sh}} \quad (5)$$

where V_o is the shunt resistance voltage and I_d is the diode current which can expressed using diode current expression in (6);

$$I_d = I_o \left[e^{\frac{qV_{oc}}{nKT}} - 1 \right] \quad (6)$$

The current generated light or solar radiation can be obtained using (7)

$$I_L = \frac{G}{G_{ref}} \times (I_{Lref} + \alpha_{Isc}(T_c - T_{cref})) \quad (7)$$

Where G is the radiation (W/m²), G_{ref} is the radiation under standard condition 1000 W/m², I_{Lref} is the photoelectric current under standard condition 0.15 A, T_{cref} is module temperature under standard condition 298 K, α_{isc} is the temperature coefficient of the short-circuit current (A/K) = 0.0065/K, and I_L is the light generated current (Radiation).

In most literature, n in (6) is an ideal value between 1 and 2, K is the Boltzmann constant, which is 1.38×10^{-9} J/K, T is the operating temperature given by (8).

$$T = T_a + \frac{T_N - 20}{800} Gc \quad (8)$$

T_a is the ambient air temperature, c and T_N is the nominal operating temperature of the PV cell. Often, c is assumed. Therefore, T_N can be expressed using (9).

$$T_N = T - T_a + (0.035)Gc \quad (9)$$

q (6) is the electron which is 1.6×10^{-9} . V_{oc} is the open circuit voltage which is sensitive to temperature and can be obtained via (10).

$$V_{oc} = \left(\frac{KT}{q}\right) \ln \frac{I_L - I_o}{I_L} \quad (10)$$

Then, the output current and voltage from the solar panel are derived as a function of time. The output power of the cell can be obtained in a similar way using (11).

$$P = FIV \quad (11)$$

where F is the cell fill factor and this can be formulated using (12);

$$F = \frac{V_o - \ln\left(\frac{V_{oc}}{q}\right) \ln\left(\frac{qV_{oc}}{KT} + 0.72\right)}{V_o + \frac{KT}{q}} \quad (12)$$

2.2.4. Battery System Model

A battery system is essential in this arrangement. This is a type of electrochemical energy storage device that stores and converts excess electrical energy (DC) from the solar panel or grid in form of electrochemical for later usage. However, each battery technology has separate ways in which it must be treated. Majorly, the mathematical modelling of a battery system in a hybrid system depends on the battery state of charge (SOC), the depth of discharge (DOD), and the state of health (SOH) [34]. The SOC is the cumulative sum of charge or discharge transfers of the battery daily. The mathematical model of the battery, the fitted controller, and the converter is model according to the following equations given in [35-38]. The size of the battery can be derived using (13).

$$S_b = N_b \times E_{BAT} \quad (13)$$

where,

$$E_{BAT}(t) = E_{BAT}(t-1) - E_{CC-OUT}(t) \times \eta_{CHG} \quad (14)$$

From (13), S_b is the size of the battery, and N_b stands for the total number of batteries within the battery bank. $E_{BAT}(t)$ is the energy stored in battery per hour (t), kWh, $E_{BAT}(t-1)$ is the energy stored in a battery at hour t-1, kWh. E_{CC-OUT} is the hourly energy output from the charge controller kWh, and η_{CHG} is the battery charging efficiency.

Also, the available energy within the battery bank during the discharge at any time, t, can be model as (15) from (14)

$$E_{BAT}(t) = E_{BAT}(t-1) - E_{Needed}(t) \quad (15)$$

$E_{Needed}(t)$, is the energy needed at a particular period of time.

The Depth of Discharge, (DOD), which is a measured as the percentage of how much energy can be withdrawn from the battery, can also be model as;

$$DOD = (1 - d) \times 100 \quad (16)$$

$$SOC_{Min} = 1 - \frac{DOD}{100} \quad (17)$$

Where d is the ratio of minimum allowable SOC voltage limit to the maximum SOC voltage across the battery terminals when fully charged. SOC_{Min} , is the minimum state of charge of the battery bank.

Therefore, the power available within the battery bank is mathematically modelled as;

$$P_{BAT,Avail}(t) = \frac{E_{BAT}(t)}{\Delta t} - SOC_{Min} \quad (18)$$

Δt , is the simulation step time.

Furthermore, the overall lifetime using the battery can be expressed using (19) according to [28].

$$R_{bat} = \min\left(\frac{N_b \times Q_{lifetime}}{Q_{thrpt}}, R_{bat,f}\right) \quad (19)$$

From (18), the lifetime throughput of a single battery measured as kWh is expressed as $Q_{lifetime}$, the yearly battery throughput measured as kWh/annum is Q_{thrpt} , while the battery float life (annum) is expressed as $R_{bat,f}$. Furthermore, the HOMER software used (20) to calculate the autonomy number of days which a fully charged battery can supply the fully loaded BS before running out of power without any input from any other power sources from the HPS [16, 28].

$$A_{batt} = \frac{N_{batt} \times V_{nom} \times Q_{nom} \left(1 - \frac{SOC_{min}}{100}\right) (24h/d)}{L_{prim-avg} (1000Wh/kWh)} \quad (20)$$

Where N_{batt} stand for the total number of batteries within the battery pack. The single battery's nominal voltage is represented by V_{nom} . The nominal capacity of an individual battery within a battery pack is represented by Q_{nom} , while the daily average load of a BS is represented by $L_{prim-avg}$.

The battery capacity is calculated using (21) according to [24].

$$C = \frac{P \times A_{batt} \times t}{V_b \times K_b \times DoD} \quad (21)$$

Where the battery capacity is represented by C measured (Ah), A_{batt} is the autonomy backup day, DoD is the depth of discharge (80%), K_b is the coefficient of the battery (1.14), P is the capacity of the total DC power load, t is the working time per day of the load (24hrs), and the voltage of the battery is represented by V_b .

2.2.5. Charge Controller and Converter Models

The aim of the charge controller is to prevent overcharging of the battery system. It also serves battery management unit. It is expressed mathematically by (22) and (23).

$$E_{CC-OUT}(t) = E_{CC-IN}(t) \times \eta_{CC} \quad (22)$$

$$E_{CC-IN}(t) = E_{REC-OUT}(t) + E_{SUR-DC}(t) \quad (23)$$

Where E_{CC-OUT} , is the hourly energy output from the charge controller, kWh. E_{CC-IN} , is the hourly energy input to charge controller, measured in kWh. η_{CC} , is the efficiency of the charge controller. $E_{REC-OUT}(t)$, is the hourly energy output from rectifier measured in kWh. And, $E_{SUR-DC}(t)$ is the amount of surplus energy from DC sources measured in kWh.

Just like the controller, the converter which holds both rectifier and inverter is necessary. The advantage of adding this rectifier is to convert the AC power from the grid to DC power of constant voltage. This grid will also power the BS, while also charging the power bank i.e. battery bank. The mathematical model for this converter is given below;

$$E_{REC-OUT}(t) = E_{REC-IN}(t) \times \eta_{REC} \quad (24)$$

where;

$$E_{REC-IN}(t) = E_{SUR-AC}(t) \quad (25)$$

Therefore, at any time t,

$$E_{SUR-AC}(t) = E_{GRID}(t) - E_{LOAD}(t) \quad (26)$$

Where $E_{REC-OUT}(t)$, is the hourly energy output from the rectifier, kWh, $E_{REC-IN}(t)$, is the hourly energy input to the rectifier, kWh, η_{REC} , is the efficiency of the rectifier. $E_{SUR-AC}(t)$, is the excess energy from AC sources, kWh, and $E_{GRID}(t)$, is the hourly energy supplied by the grid.

2.3. Costs Modelling

In HOMER software, the total Net Present Cost (NPC) of a system is the present value of all the costs the system incurs over its lifetime, minus the present value of all the revenue it earns over its lifetime. NPC includes capital costs, replacement costs, O&M costs, fuel costs, emissions penalties, and the costs of buying power from the grid. Thus, the NPC can be mathematically expressed [39] using (27).

$$NPC = \frac{TAC}{CRF} \quad (27)$$

The Total Annualized Cost (TAC) is the annualized value of the total NPC and the Capital Recovery Factor (CRF), is expressed by [39], using (28).

$$CRF = \frac{i(1+i)^n}{(1+i)^n - 1} \quad (28)$$

In (28), i is the annual real interest rate, while n is the project lifetime. According to HOMER, all prices increase directly at the same rate while nominal interest rate was used instead of annual real interest [16].

Other costs include the discount factor f_d . Discount factor is used to calculate the present value of a cash flow that occurs in any year during the project's lifetime [28, 39].

$$f_d = \frac{1}{(1+i)^n} \quad (29)$$

Salvage cost is the power systems components value remaining at the end of completion of a particular project's lifetime. HOMER calculated salvage cost using (22)[28].

$$S = rep \left(\frac{rem}{comp} \right) \quad (30)$$

In (30), rep is the replacement cost of the component, rem is the remaining lifetime of the component, while $comp$ is the lifetime of the component. The operating cost is the annualized value of all costs and revenues other than initial capital costs. HOMER uses (31) to calculate the operating cost.

$$C_{operating} = C_{ann,tot} - C_{ann,cap} \quad (31)$$

Where $C_{ann,tot}$ is the total annualized cost, and $C_{ann,cap}$ is the total capital cost. Levelized cost of energy (COE) is the average cost per kWh of useful electrical energy produced by the system. HOMER modelled it using (32).

$$LCOE = \frac{\sum_{t=1}^n \frac{I_t + M_t + F_t}{(1+r)^t}}{\sum_{t=1}^n \frac{E_t}{(1+r)^t}} \quad (32)$$

Where the electricity generation per annum is E_t , F_t is the fuel expenditures per annum, I_t is the investment expenditures per annum, M_t is the operation and maintenance expenditures per year, while, r , is the discount rate per annum. The PV system life is taken as 25 years at the discount rate is 6 %, and the system life rate is 10 years.

3. Methodology

The aim of this section is to give the site description, the data modelling, the BS load profile parameters, architecture layout as well as the cost and features of components used during the simulation. It is important to have these data to generate the power needed at the lowest cost of operation.

3.1. Site Description, Solar Resources, and Clearance Index

Statistical modelling was carried out on solar irradiation data collected from two weather stations within Gauteng province i.e. Johannesburg and Pretoria. These were analysed for the use of the BS located in Soshanguve. Soshanguve is a township located in about 45 km north of Pretoria under the Gauteng province, South Africa. It lies between the latitude and longitude of 25.5226° S and 28.1006° E respectively. Figure 4 is the map of Soshanguve.



Figure 4. Map of Soshanguve

The average monthly solar data resources over the period of ten years considered are shown in Figure 5.

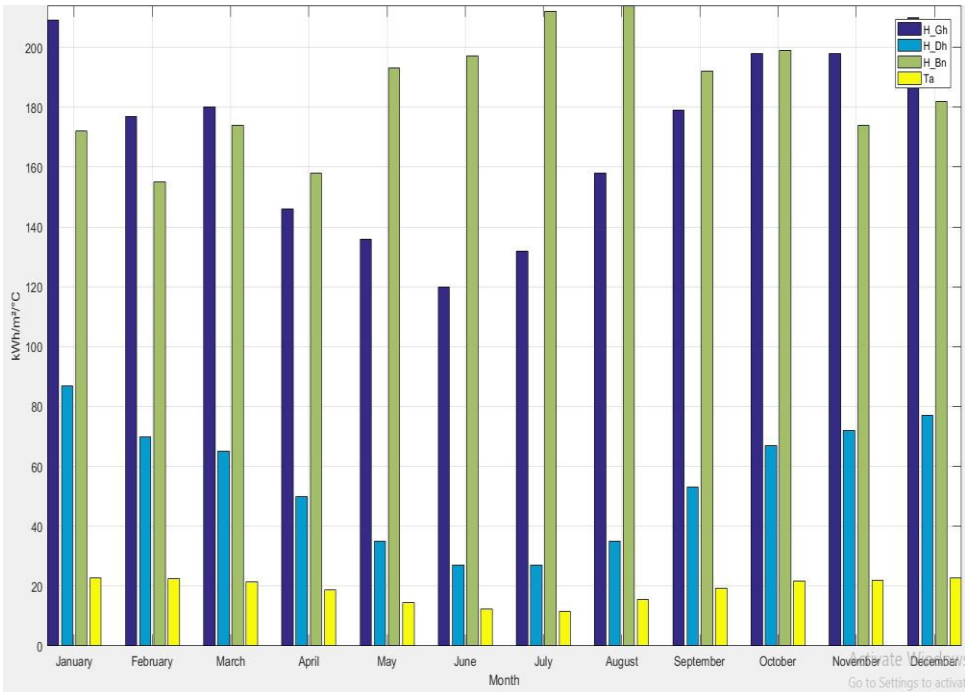


Figure 5. Average Monthly Solar data of Pretoria, South Africa.

The average monthly solar radiation data used in this work is presented in Figure 5 and 6. Furthermore, Figure 6, shows the average daily solar radiation for this town of Soshanguve to be about 5.4645 kWh/m², while the average daily clearness index calculated was 0.605 using (33).

$$K_T = \frac{H_{ave}}{H_{o,ave}} \quad (33)$$

Where H_{ave} is the average month radiation on the horizontal surface of the earth $\left[\frac{kWh}{m^2 \cdot day}\right]$, and $H_{o,ave}$ is the extraterrestrial horizontal radiation- radiation on a horizontal surface at the top of the Earth's atmosphere $\left[\frac{kWh}{m^2 \cdot day}\right]$ [24]. The solar intensity of solar radiation at the top of the earth's atmosphere is;

$$G_{on} = G_{sc} \left(1 + 0.33 \cos \frac{360n}{365}\right) \quad (34)$$

where

$$G_{sc} = \text{Solar constant} \left[\frac{1.367kW}{m^2}\right] \quad (35)$$

And n is the day in a year from 1 to 365 days.

Both clearness index and daily radiation values further confirmed that this site is suitable to produce sufficient solar energy. This is when these values are compared to other location such as South Korea with an average monthly radiation of 4.01 kWh/m²/day, and clearness index of 0.504 and are currently using solar PV powered BSs [21]. These values and a comprehensive pre-feasibility study are important for efficient and reliable designing of this HPS. Furthermore, for a solar energy harvesting form of renewable energy to power an off-grid BS, meteorological data are critical for efficient sizing.

Figure 6 shows the graphical illustration of the average monthly solar resources profile used in this study. The average monthly daily radiation is represented with a bar chart in orange colour, while the blue line represented the average monthly daily clearance index. The highest average daily radiation of 6.763 kWh/m²/day is experienced in November, while the lowest is in June with radiation of 3.796 kWh/m²/day. The monthly variation is due to change in weather season. This value will assist in proper designing, sizing and forecasting, thus reduces any chance of downtime as a result of a power outage. This means the designed system will be able to supply the energy requirement by the BS.

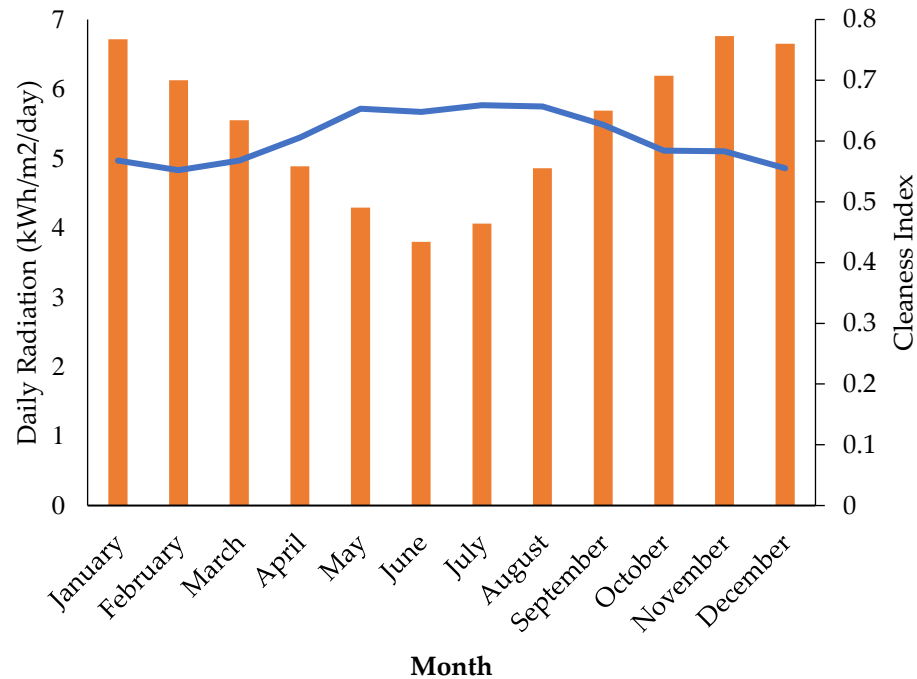


Figure 6. Average Monthly Daily Global Horizontal Radiation (GHI) and clearness index

3.2. Base Station Load Profile

The efficiency of a solar-powered mobile cellular BS principally depends on the 24 hrs daily load profile of that BS. Hence, sizing, designing, reliability as well as modelling of HPS critically hangs on BS load. Therefore, a 24hr daily electrical load or power consumption of a mobile cellular BS situated on this site in Soshanguve was obtained using (1). Thus, it was used in this modelling. Figure 7 shows the daily load consumption profile for this BS over the period of 24 hrs. Figure 8 shows the average seasonal load consumption for this mobile cellular BS per year. For this calculation, HOMER uses 24 hrs power consumption load profile over a period of 365 days to safeguard accuracy in the analysis using (1) and (2).

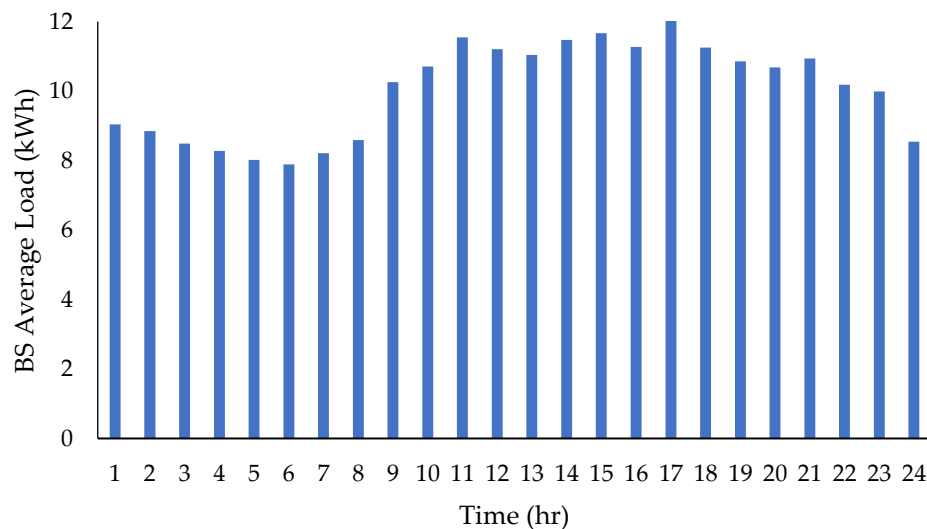


Figure 7. 24 hrs Average Daily BS Load Consumption Profile

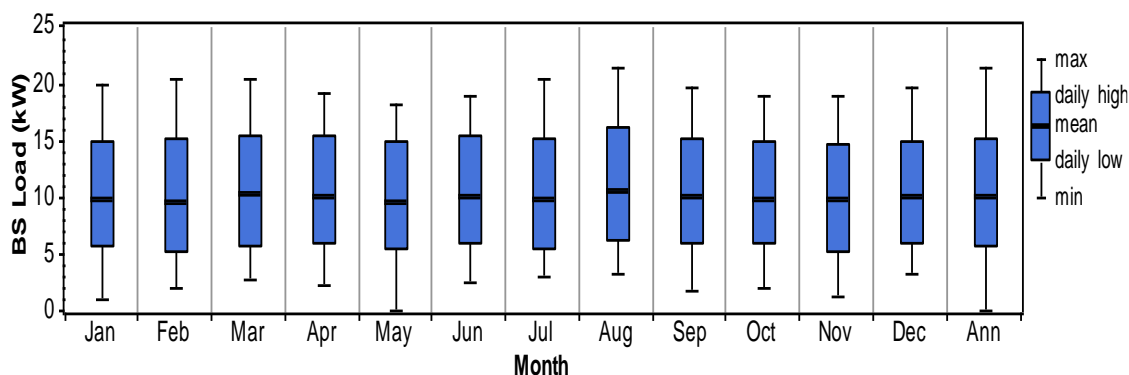


Figure 8. BS Average Seasonal Load Profile.

3.3. System Configuration and Simulation

The aim of this section is to provide the architecture layout of the HPS as well as the parameters of the components' used in this simulation.

3.3.1. Solar PV Standalone BS Configuration

Through HOMER software, the solar PV stand alone, and hybrid power system was designed, modelled, and simulated for a mobile cellular base station in this study, using an average daily solar radiation value of 5.4645 kWh/m² and daily clearance index of 0.605 as a benchmark. Figure 11 shows the schematic configuration of this HPS arrangement that comprises a mobile cellular BS, solar PV modules, and a battery pack. Figure 2 shows the summary of the energy control algorithm flowchart for this simulation. The function of this power source control algorithm is to figure out, prioritize, and select the available source from the solar PV, the battery system and the backup generating set HPS. By this configuration, there will be no downtime in the operation of the BS. Fuzzy logic control in Matlab-Simulink was also used in implementing the power source management algorithm flow chat in Figure 2. Figure 9 shows the designed model in Simulink, while the fussy logic control implementation is shown in power source management arrangement in Figure 10. Both HOMER and Matlab/Simulink designed and simulation analysis reveals that PV array approximated rated needed is 76 kW using (4) and the number of battery units needed is 208 using (5). The output of the PV module varies based on both input ambient and the solar irradiation. The mathematical modelling of this PV module used is described by modelling (5) to (12) in Matlab/Simulink. Therefore, 220 scenarios were simulated using HOMER software, the result obtained showed the best HPS configuration in terms of energy production, environmental benefits, and lowest cost that is most suitable for this standalone solar PV powered mobile cellular BS. The cost implication and the technical specifications of the components used in the simulation for solar PV standalone BS model in HOMER are given in Table 1. The costs are mathematically modelled using (27) to (32).

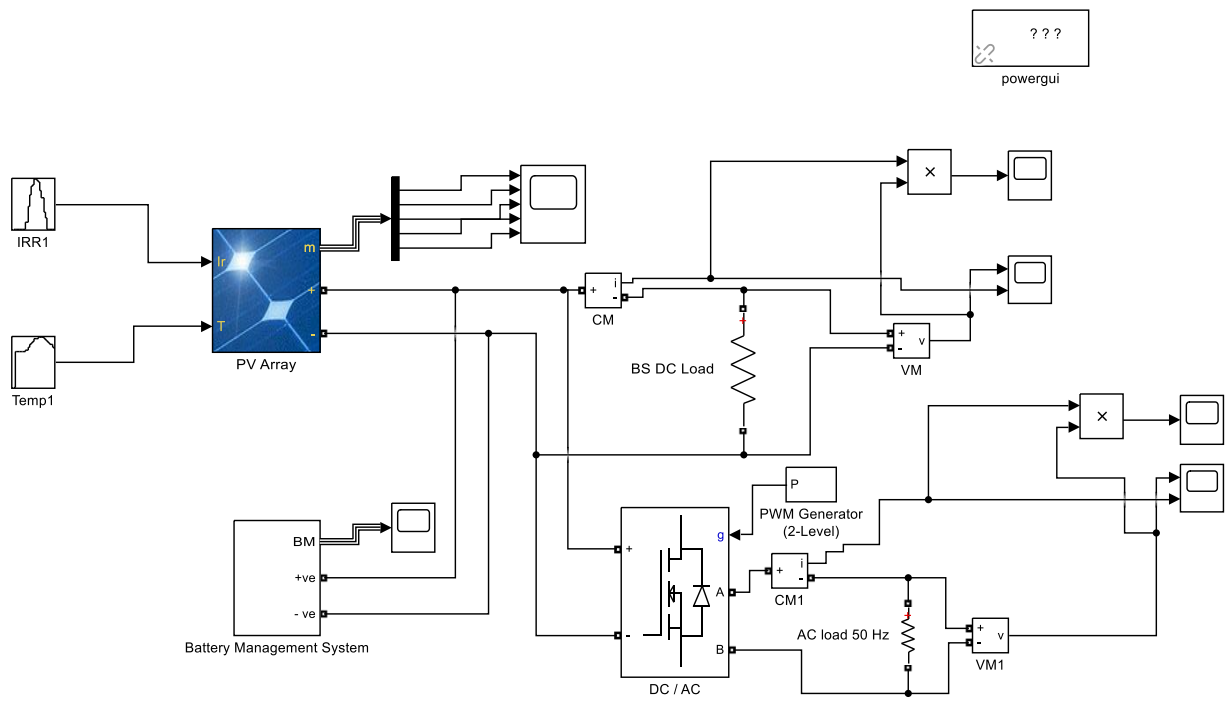


Figure 9. Designed Hybrid Power System Management in Matlab/Simulink

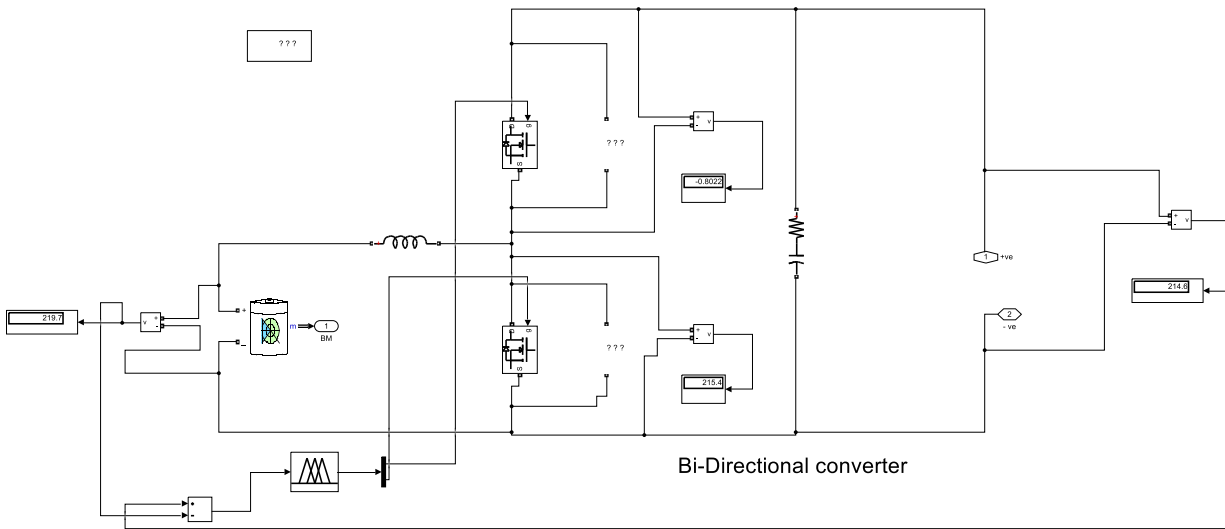


Figure 10. Fuzzy logic controlled power source management in Matlab/Simulink

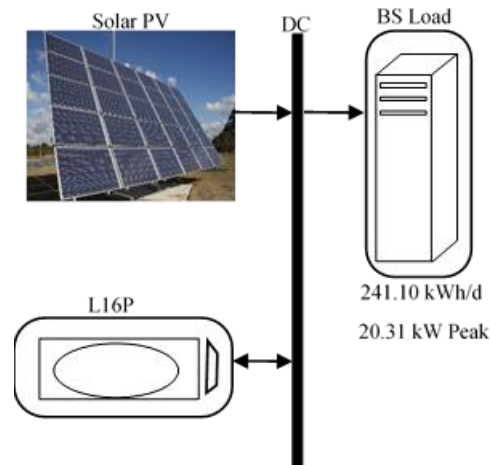


Figure 11. Schematic diagram of a standalone solar PV powered Mobile Cellular BS

Table 1: Cost and parameters of the used components for Solar PV stand alone

Component	Capital (\$)	Replacement (\$)	O&M (\$)	Fuel (\$)	Salvage (\$)	Total (\$)	Parameters	Annual Production
Generic flat Plate PV	75,625	0	9,776.43	0	0	85,401.43	75.6 kW	146,847 kWh
Trojan L16P	62,400	88,043.88	26,889.23	0	6,922.51	170,410.61	208 units	50,526 kWh
System	138,025	88,043.88	36,665.66	0	6,922.51	255,812.04		
Total NPC						255,812.00		
Levelized COE						0.2250		
Operating Cost						9,111.34		

For this solar PV standalone power source simulation, the generic flat-plate PV module of 75.6 kW capacity rating was used based on (4). Table 2 shows the technical specification of the generic flat plate solar PV module used in this model. The total yearly energy contribution of this PV array is 146,847 kWh obtained using (4).

Table 2: Features of standalone generic flat plate solar PV module

Quantity	Value	Units
Rated Capacity	75.6	kW
Mean Output	16.8	kW
Mean Output per day	402	kWh/d
Capacity Factor	22.2	%
Total Production	146,847	kWh/yr.

The second item for this standalone model is the energy storage device known as a battery. L16P battery model which was designed by Trojan company is used in this design. This has 26 parallel strings connected to 48V bus voltage. The nominal rated voltage of the trojan L16P battery is 6V, hence 48V DC bus-bar connected in series was used. Furthermore, with 208 units of battery operating at a nominal

voltage of 6 V, its annual energy production is 50,526 kWh obtained using (21). From (20), the battery can supply the BS load independently for 47.4 hr which is approximately 2 days autonomy. Other technical parameters are summarized in Table 3 obtained using the mathematical models from (13) to (21). Apart from the cost benefits, this standalone arrangement produces no GHG emission. The expected life of this battery arrangement is approximately 7.07 years calculated using (19).

Table 3: Trojan L16P battery for solar PV standalone

Quality	Value	Units
Batteries	208	Qty
String Size	8.00	Batteries
Strings in Parallel	26.0	Strings
Bus Voltage	48.0	Volt
Autonomy	47.4	Hr
Storage Wear Cost	0.195	\$/kWh
Nominal Capacity	595	kWh
Usable Nominal Capacity	476	kWh
Lifetime Throughput	357, 136	kWh
Expected Life	7.07	Yr.

3.3.2. HPS with Diesel GenSet Configuration

Apart from the solar PV stand-alone, a hybrid possibility with diesel genset was considered. The schematic diagram is given in Figure 12 using the same BS load, and solar resources. The cost and parameters of the components used for this arrangement are given in Table 4. Likewise, from the simulation carried out using HOMER software, the best arrangement in terms of the components parameters and cost efficiency was chosen from many scenarios created.

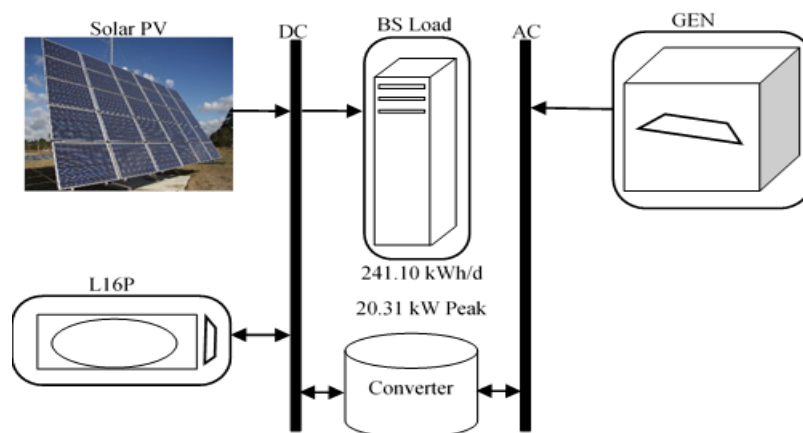


Figure 12. Schematic diagram of HPS with Diesel Gen set for a BS

Table 4: The cost of components and parameters for HPS with diesel GenSet

Component	capital (\$)	Replacement (\$)	O&M (\$)	Fuel (\$)	Salvage (\$)	Total (\$)	Parameters	Production
Autosize GenSet	12,500	0	3,432.26	14,896.06	1,227.73	29,600.59	25.0 kW	3,082 kWh
Generic flat Plate PV	56,390.24	0	7,289.86	0	0	63,680.09	56.4 kW	109,498 kWh
System Converter	3,369.78	1,429.71	0	0	269.09	4,530.41	11.2 kW	0.317 kW
Trojan L16P	43,200.00	88,789.23	18,615.62	0	156.04	150,448.81	144 units	49,300 kWh
System	115,460.02	90,218.94	29,338	14,896.06	1,652.86	248,259.90		
Total NPC						248,259.90		
Levelized COE						0.22		
Operating Cost						10,272.65		

For this GenSet of 25 kW, Table 5 summarized the overall fuel consumption and its features.

Table 5: Autosize GenSet diesel consumption and features

Autosize GenSet Diesel Consumption		
Quantity	Value	Units
Total fuel consumed	1,152	L
Avg fuel per day	3.16	L/day
Avg fuel per hour	0.132	L/hour
Hours of Operation	354	Hrs/yr.
Number of Starts	48.0	Starts/yr.
Operational Life	42.4	Yr.
Capacity Factor	1.41	%
Fixed Generation Cost	2.65	\$/hr
Marginal Generation Cost	0.251	\$/kWh
Electrical Production	3,082	kWh/yr.
Mean Electrical Output	8.71	kW
Minimum Electrical Output	6.25	kW
Maximum Electrical Output	12.5	kW

The solar PV used in this HPS is a Generic flat plate solar PV module. It has a rated capacity of 56.4 kW and total energy production is 109,498 kWh per annum obtained using (4). Figure 12 is the average monthly electrical energy production by the solar PV module. Other parameters are summarized in Table 6.

Table 6: Features of Generic flat plate solar PV

Quantity	Value	Units
Rated Capacity	56.4	kW
Mean Output	12.5	kW
Mean Output per day	300	kWh/d
Capacity Factor	22.2	%
Total Production	109,498	kWh/yr.

The system converter used in this arrangement with capacity and price as given in Table 4. Converter contains both inverter and rectifier with a capacity of 11.2 kW and 10.7 kW respectively. The annual total electric energy production is obtained using (23) to (26) to 0.317 kW. Other parameters are summarized in Table 7.

Table 7: Capacity of Converter

Quantity	Inverter	Rectifier	Units
Capacity	11.2	10.7	kW
Mean Output	0	0.317	kW
Minimum Output	0	0	kW
Maximum Output	0	11.2	kW
Capacity Factor	0	2.82	%

The energy storage used in this simulation is Trojan L16P battery. With a nominal voltage of 6 V, connected over 48 V bus bar, a total number of 144 batteries were used in this designed. Using (21), its annual electrical energy production is 49,300 kWh. The battery has an autonomy for 32.8 hr by which it can supply the BS load independently using (20). Table 8 summarized the capacity and characteristics of the battery.

Table 8: Capacity and characteristics of Trojan L16P

Quality	Value	Units
Batteries	144	Pcs
String Size	8.00	Pcs
Strings in Parallel	18.0	Pcs
Bus Voltage	48.0	Volt
Autonomy	32.8	Hr
Storage Wear Cost	0.195	\$/kWh
Nominal Capacity	412	kWh
Usable Nominal Capacity	330	kWh
Lifetime Throughput	247,248	kWh
Expected Life	5.02	Yr.

4. Results and Discussion

This section discusses the result of the simulation from the architectural layout and sizing of the components used in this design in section 3.

Figure 13 shows the characteristic of the PV module in P-V curves simulated in Matlab/Simulink. The model was simulated under average hourly ambient temperature and solar irradiation of the BS site location as an input. The result shows an increase in PV energy output as the solar irradiance increase depending on the hour of the day. Therefore, both the voltage and the current drawn from the PV modules increases as the solar irradiance increase, but decreases when there is an increase in ambient temperature and vice versa. Therefore, there is a decrease in the output power as the ambient temperature increases and solar irradiance decreases. Figure 11 also shows a reduction in both voltage and current output of the PV module due to an increase in input ambient temperature.

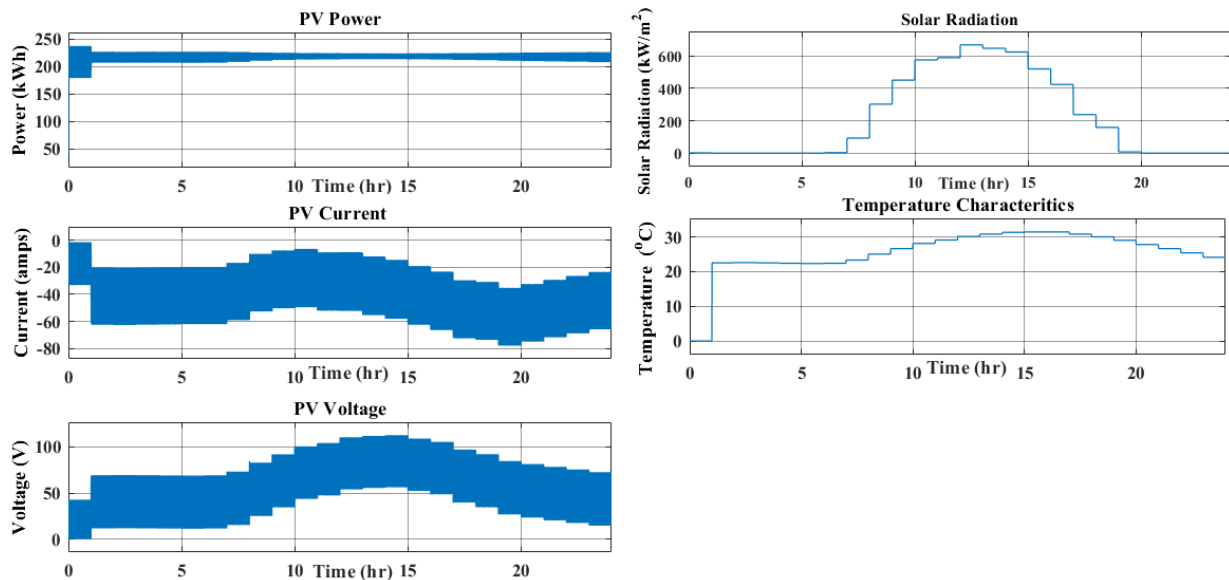


Figure 13. The average hourly PV array I-V characteristics.

Figure 14 shows the battery management Fuzzy logic controller implemented in this in this model shown in figure 10. This depends on the battery's state of charge (SOC). This allows the battery not to discharge below 50 % and not to overcharge above 100 % depending on the average daily hourly solar irradiance and the load of the mobile cellular BS

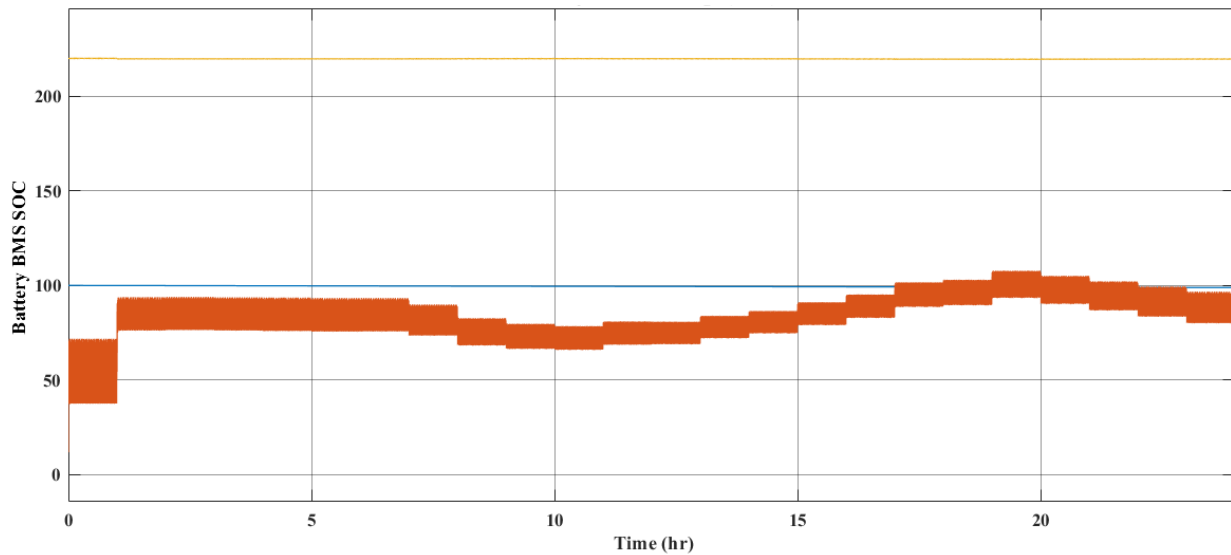


Figure 14. Average hourly battery management SOC

Figure 15 is a graph of an average monthly time series load consumption of the standalone BS used. This shows an annual load consumption of 87,929 kWh using (1). Using an average daily solar radiation of 5.465 kWh/m² and all the parameters provided in subsection 3.3.1, Figure 16 reveals the energy production by the solar PV to supply the daily load consumption of the BS with the result displayed in Figure 15. The result shows an annual total energy production of 146,847 kWh/yr using (4). by the generic flat plate PV array operating at 4,384 hrs/yr in a standalone arrangement and 109,498 kWh for HPS arrangement using HOMER. With the BS load of 87,929 kWh per year obtained using (1) and (2), there will be excess electricity of about 47,756 kWh per year. This excess energy will be used in case of an increase in load consumption, while the remaining will be stored in the battery for future usage. Figure 16 shows the monthly electric energy production of the solar PV module. Figure 16 further confirms the possibility of using the solar PV to achieve 100 % renewable energy penetration. Consequently, the quantity of GHG produces for this standalone solar PV is zero, thus making it ideal for the elimination of GHG emission as compared to the exclusive use of diesel gen set or the HPS of PV-Battery-GenSet configuration. Figure 17 shows the average monthly percent of SOC of the batteries.

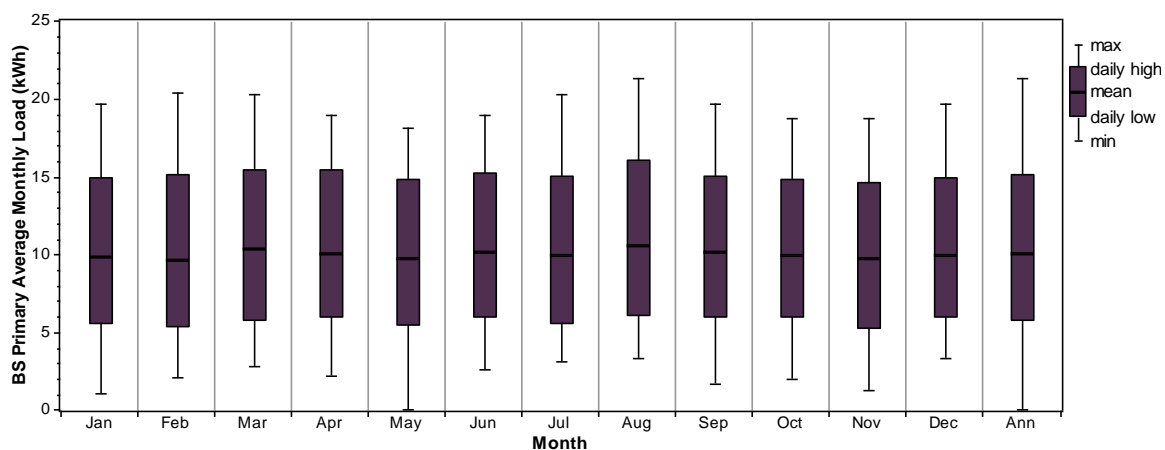


Figure 15. Time Series Average BS Monthly Load Consumption

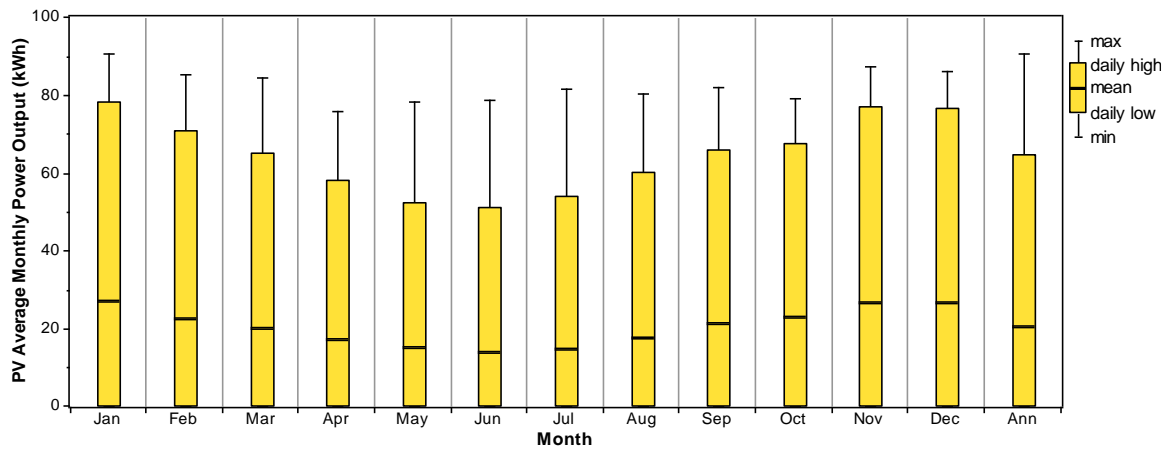


Figure 16. Average Monthly Electric Production by the PV Module

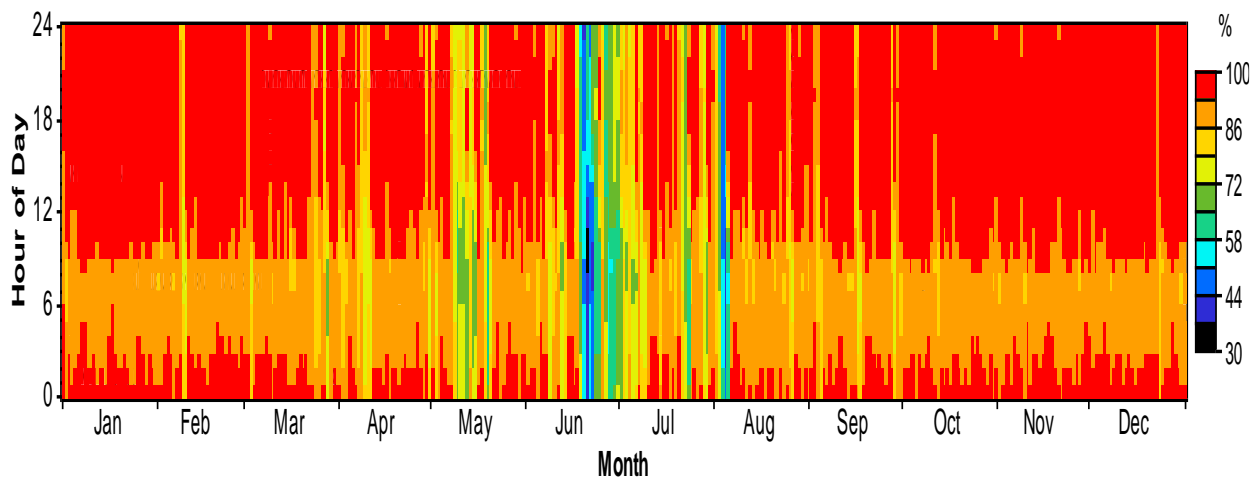


Figure 17. Average Monthly Percent of SOC of the Batteries

The Trojan L16P batteries used gave an annual throughput of 50,526 kWh/yr, with an energy input of 56,355 kWh/yr, the output of 45,192 kWh/yr and losses of 11,284 kWh/yr due to ageing. Figure 18 is the DMap of the energy content of the battery in time series in average hourly values of the PV array power output with SOC over a period of 12-months for the solar-powered mobile cellular BS. The lowest percent of charge is experienced in the month of March and June, while the highest is in the month of January and November with daily GHI of 6.716 kWh/m²/day and 6.763 kWh/m²/day respectively as displayed in Figure 19. Figure 19 further reveals that the battery bank is at average maximum 45 % of the year and minimum at less than 1 % of the year.

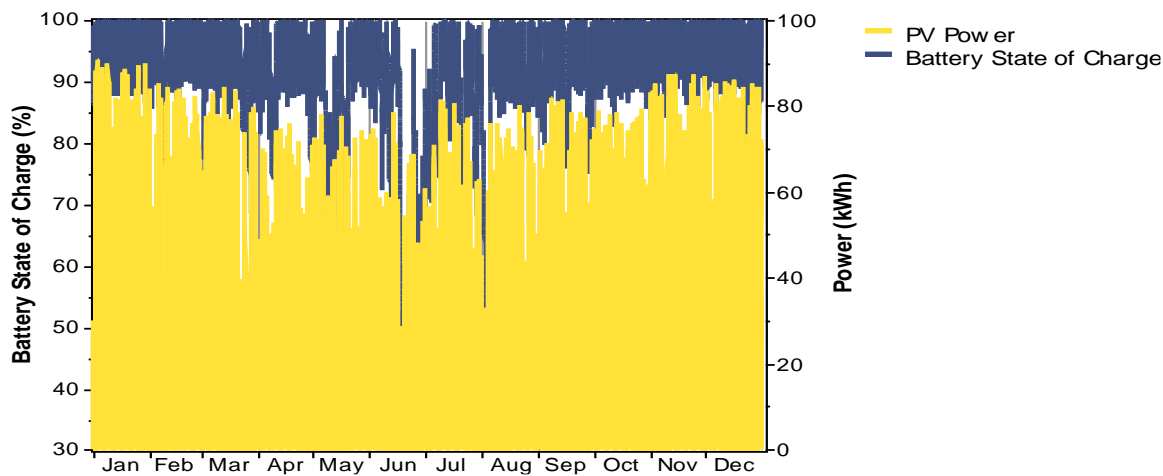


Figure 18. Trojan L16P average monthly energy content in time series.

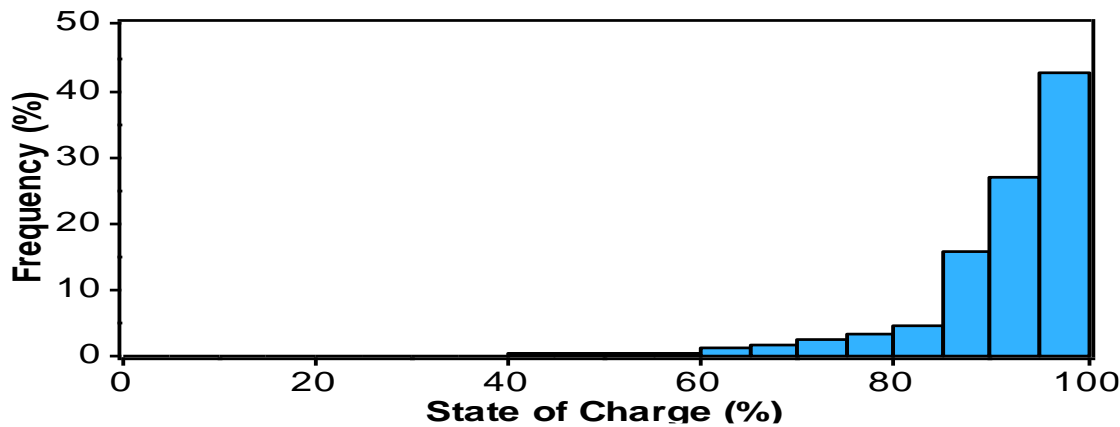


Figure 19. The average yearly frequency for battery state of charge

For the HPS with GenSet in subsection 3.3.2, the total energy produced is 112,579 kWh/yr between the generic flat plate PV and the GenSet. From Figure 20, the GenSet could support the BS when there is low production from the PV because of low GHI especially in the months of March and June. However, this arrangement emits 3061.235 kg/yr of GHG. The breakdown of the GHG emission is summarized in Table 9.

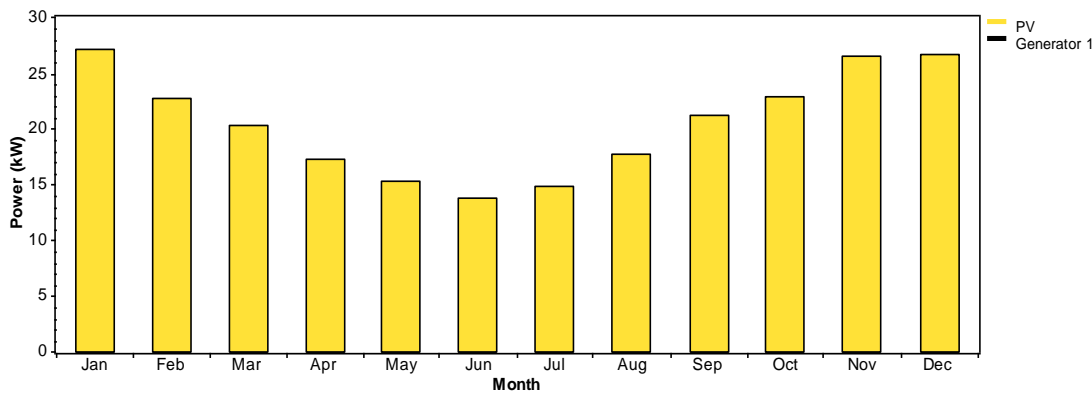


Figure 20. Average monthly electrical energy contribution by HPS.

Table 9: GenSet GHG Emission

Autosize GenSet GHG Emission		
Quantity	Value	Units
Carbon Dioxide	3,016	kg/yr.
Carbon Monoxide	19	kg/yr.
Unburned Hydrocarbons	0.83	kg/yr.
Particulate Matter	0.115	kg/yr.
Sulphur Dioxide	7.39	kg/yr.
Nitrogen Oxides	17.9	kg/yr.
Total	3061.2 35	Kg/yr

Comparing these results to the use of GenSet as given in Table 10, the HPS is more economically viable and environmentally friendly as it will eliminate 90,295 kg of GHG per year. This result can be used as a feasibility guide in planning the energy production.

Table 10: Cost comparison and GHG emission

Architecture	Costs				Energy Production (kWh)	GHG Production (kg/yr.)
	Levelized COE (\$)	Initial Capital (\$)	Operating Cost (\$)	NPC (\$)		
Solar PV standalone with batteries	0.225	138,025	9,111	255,812	197,373	0
HPS with Gen Set	0.218	115,460	10,273	248,260	161,880.32	3061.235
Gen Set Alone	0.557	17,973	47,624	633,633	98,054	90,295.9

5. Conclusion

This research work examined the cost, technical and environmental benefits that can be derived from the use of renewable energy source to power a selected mobile cellular BS site in Soshanguve rural area of South Africa. The simulation used the solar resource of this location collected from NASA and modelled statistically to figure out the technical feasibility of using the solar energy as a primary energy source, without power shortage at this mobile cellular BS.

Thus, the statistical modelling done using solar radiation resource exposure character pattern of Pretoria, South Africa, revealed an average annual daily solar radiation of 5.4645 Wh/m²/d and 0.605 clearness index. The simulation and the design were done using the Hybrid Optimization Model for Electric Renewables (HOMER) software and Matlab/Simulink. The simulation finding shows that the HPS of solar PV-battery combination has total Net Present Cost (NPC), Levelized Cost of Energy (COE), and Operating cost of \$255,812, \$0.23, and \$9,111 respectively clean energy as against the conventional HPS of diesel generator which has total Net Present Cost (NPC), Levelized Cost of Energy (COE), and

Operating cost of \$248,260, \$0.22, \$10,273 respectively, but 3061.235 kg/yr of GHG emission. As against conventional BS powered with Gen Set-Battery of total Net Present Cost (NPC), Levelized Cost of Energy (COE), and Operating cost of \$633,633, \$0.559, \$47,624 respectively, with the GHG emission of 90,295.9 kg/yr. It can be concluded that the architecture of solar PV standalone is more economical and environmental friendly with zero emission of GHG compared to another layout like diesel gen set alone, or HPS with gen set to power the BS as shown in section 4. The cost comparison summary is given in Table 10 over the period of 25 years. The result clearly indicates a superior environmental friendliness, technical, and cost-effectiveness are achievable through the use of renewable energy source. Although the use of GenSet alone had lowest initial capital, its cost of operation is huge compared to other HPS discussed. Furthermore, its high emission of GHG cannot be taken lightly, thus renewable standalone gave a better option in terms of cost and emission of GHG.

Acknowledgements: The authors acknowledge the research supports received from the Tshwane University of Technology, Pretoria and the Council for Scientific and Industrial Research (CSIR), Pretoria, South Africa.

6. References

- [1] Cisco, "Visual Networking Index Forecast Projects Nearly 11-Fold Increase In Global Mobile Data Traffic From 2013 To 2018," Cisco Public, San Francisco, CA, USA2014.
- [2] V. K. Bhargava and A. Leon-Garcia, "Green cellular networks: A survey, some research issues and challenges," in *Communications (QBSC), 2012 26th Biennial Symposium on*, 2012, pp. 1-2: IEEE.
- [3] K. Kusakana and H. J. Vermaak, "Hybrid renewable power systems for mobile telephony base stations in developing countries," *Renewable Energy*, vol. 51, pp. 419-425, 3// 2013.
- [4] M. Meo, E. Le Rouzic, R. Cuevas, and C. Guerrero, "Research challenges on energy-efficient networking design," *Computer Communications*, vol. 50, pp. 187-195, 2014.
- [5] S. Lambert, W. Van Heddeghem, W. Vereecken, B. Lannoo, D. Colle, and M. Pickavet, "Worldwide electricity consumption of communication networks," *Optics Express*, vol. 20, no. 26, pp. B513-B524, 2012.
- [6] V. Chamola and B. Sikdar, "Solar powered cellular base stations: current scenario, issues and proposed solutions," *IEEE Communications Magazine*, vol. 54, no. 5, pp. 108-114, 2016.
- [7] A. Aris and B. Shabani, "Sustainable Power Supply Solutions for Off-Grid Base Stations," *Energies*, vol. 8, no. 10, p. 10904, 2015.
- [8] A. Fehske, G. Fettweis, J. Malmudin, and G. Biczok, "The global footprint of mobile communications: The ecological and economic perspective," *IEEE Communications Magazine*, vol. 49, no. 8, 2011.
- [9] M. Webb, "SMART 2020: Enabling the low carbon economy in the information age," *The Climate Group. London*, vol. 1, no. 1, pp. 1-1, 2008.
- [10] T. O. Olwal, K. Djouani, and A. M. Kurien, "A survey of resource management toward 5G radio access networks," *IEEE Communications Surveys & Tutorials*, vol. 18, no. 3, pp. 1656-1686, 2016.
- [11] M. Alsharif and J. Kim, "Optimal Solar Power System for Remote Telecommunication Base Stations: A Case Study Based on the Characteristics of South Korea's Solar Radiation Exposure," *Sustainability*, vol. 8, no. 9, p. 942, 2016.
- [12] P. D. Diamantoulakis and G. K. Karagiannidis, "On the design of an optimal hybrid energy system for base transceiver stations," *J. Green Eng*, vol. 3, pp. 127-146, 2013.
- [13] H. Zhang, C. Jiang, X. Mao, and H.-H. Chen, "Interference-limited resource optimization in cognitive femtocells with fairness and imperfect spectrum sensing," *IEEE Transactions on Vehicular Technology*, vol. 65, no. 3, pp. 1761-1771, 2016.
- [14] H. Zhang, C. Jiang, N. C. Beaulieu, X. Chu, X. Wang, and T. Q. Quek, "Resource allocation for cognitive small cell networks: A cooperative bargaining game theoretic approach," *IEEE Transactions on Wireless Communications*, vol. 14, no. 6, pp. 3481-3493, 2015.

- [15] M. S. Okundamiya, J. O. Emagbetere, and E. A. Ogijor, "Assessment of renewable energy technology and a case of sustainable energy in the mobile telecommunication sector," *The Scientific World Journal*, vol. 2014, 2014.
- [16] M. H. Alsharif, "Techno-Economic Evaluation of a Stand-Alone Power System Based on Solar Power/Batteries for Global System for Mobile Communications Base Stations," *Energies*, vol. 10, no. 3, p. 392, 2017.
- [17] M. H. Alsharif, R. Nordin, and M. Ismail, "Energy optimisation of hybrid off-grid system for remote telecommunication base station deployment in Malaysia," *EURASIP Journal on Wireless Communications and Networking*, vol. 2015, no. 1, p. 64, 2015.
- [18] D. Zordan, M. Miozzo, P. Dini, and M. Rossi, "When telecommunications networks meet energy grids: cellular networks with energy harvesting and trading capabilities," *IEEE Communications Magazine*, vol. 53, no. 6, pp. 117-123, 2015.
- [19] O. Babatunde, M. Emezirinwune, H. Denwigwel, and J. Akin-Adeniyi, "Hybrid power system for off-grid communities: Techno-economic and energy mix analysis," in *Electro-Technology for National Development (NIGERCON), 2017 IEEE 3rd International Conference on*, 2017, pp. 946-952: IEEE.
- [20] T. O. Akinbulire, P. O. Oluseyi, and O. M. Babatunde, "Techno-economic and environmental evaluation of demand-side management techniques for rural electrification in Ibadan, Nigeria," *International Journal of Energy and Environmental Engineering*, vol. 5, no. 4, pp. 375-385, 2014.
- [21] M. H. Alsharif, "Optimization design and economic analysis of energy management strategy based on photovoltaic/energy storage for heterogeneous cellular networks using the HOMER model," *Solar Energy*, vol. 147, pp. 133-150, 2017.
- [22] G. Auer and O. Blume, "Earth project d2. 3-energy efficiency analysis of the reference systems, areas of improvements and target breakdown," *EARTH FP7*, 2011.
- [23] B. A. Aderemi, S. D. Chowdhury, T. O. Olwal, and A. M. Abu-Mahfouz, "Solar PV powered mobile cellular base station: Models and use cases in South Africa," in *AFRICON, 2017 IEEE*, 2017, pp. 1125-1130: IEEE.
- [24] P. O. Oviroh and T.-C. Jen, "The Energy Cost Analysis of Hybrid Systems and Diesel Generators in Powering Selected Base Transceiver Station Locations in Nigeria," *Energies*, vol. 11, no. 3, p. 687, 2018.
- [25] V. Chamola and B. Sikdar, "Resource provisioning and dimensioning for solar powered cellular base stations," in *2014 IEEE Global Communications Conference*, 2014, pp. 2498-2503: IEEE.
- [26] V. Chamola and B. Sikdar, "Power Outage Estimation and Resource Dimensioning for Solar Powered Cellular Base Stations," *IEEE Transactions on Communications*, vol. 64, no. 12, pp. 5278-5289, 2016.
- [27] H. Mutlu, M. Alanyali, and D. Starobinski, "Spot pricing of secondary spectrum access in wireless cellular networks," *IEEE/ACM Transactions on Networking (TON)*, vol. 17, no. 6, pp. 1794-1804, 2009.
- [28] T. Lambert, P. Gilman, and P. Lilienthal, "Micropower system modeling with HOMER," *Integration of alternative sources of energy*, pp. 379-418, 2006.
- [29] O. Babatunde, D. Akinyele, T. Akinbulire, and P. Oluseyi, "Evaluation of a grid-independent solar photovoltaic system for primary health centres (PHCs) in developing countries," *Renewable Energy Focus*, vol. 24, pp. 16-27, 2018.
- [30] V. Chamola and B. Sikdar, "Outage estimation for solar powered cellular base stations," in *2015 IEEE International Conference on Communications (ICC)*, 2015, pp. 172-177: IEEE.
- [31] N. Das and S. Islam, "Design and analysis of nanostructured gratings for conversion efficiency improvement in GaAs solar cells," *Energies*, vol. 9, no. 9, p. 690, 2016.

- [32] F. Fadakar Masouleh, N. Das, and S. M. Rozati, "Nano-structured gratings for improved light absorption efficiency in solar cells," *Energies*, vol. 9, no. 9, p. 756, 2016.
- [33] D. Akinyele, J. Belikov, and Y. Levron, "Challenges of Microgrids in Remote Communities: A STEEP Model Application," *Energies*, vol. 11, no. 2, p. 432, 2018.
- [34] D. Akinyele, J. Belikov, and Y. Levron, "Battery Storage Technologies for Electrical Applications: Impact in Stand-Alone Photovoltaic Systems," *Energies*, vol. 10, no. 11, p. 1760, 2017.
- [35] M. S. Okundamiya, J. O. Emagbetere, and E. A. Ogujor, "Techno-Economic Analysis of a Grid-Connected Hybrid Energy System for Developing Regions," *Iranica Journal of Energy & Environment*, vol. 6, no. 4, pp. 243-254, 2015.
- [36] K. Sopian, A. Zaharim, Y. Ali, Z. M. Nopiah, J. A. Razak, and N. S. Muhammad, "Optimal operational strategy for hybrid renewable energy system using genetic algorithms," *WSEAS Transactions on Mathematics*, vol. 7, no. 4, pp. 130-140, 2008.
- [37] A. Salmani, S. Sadeghzadeh, and M. Naseh, "Optimization and sensitivity analysis of a hybrid system in Kish_Iran," *International Journal of Emerging Technology and Advanced Engineering*, vol. 4, no. 1, pp. 349-355, 2014.
- [38] H. Abdolrahimi and H. K. Karegar, "Optimization and sensitivity analysis of a hybrid system for a reliable load supply in Kish_Iran," *International Journal of Advanced Renewable Energy Researches (IJARER)*, vol. 1, no. 4, 2012.
- [39] A. Chauhan and R. Saini, "A review on integrated renewable energy system based power generation for stand-alone applications: configurations, storage options, sizing methodologies and control," *Renewable and Sustainable Energy Reviews*, vol. 38, pp. 99-120, 2014.